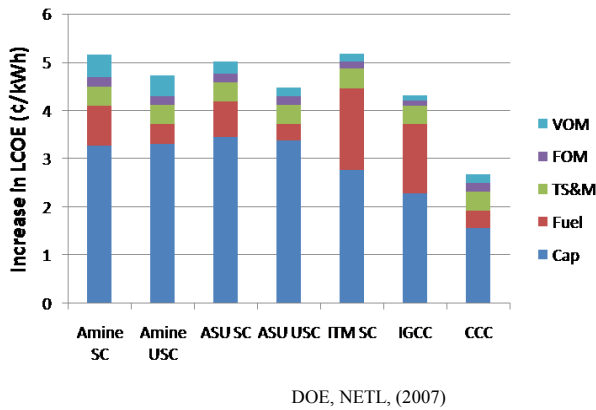


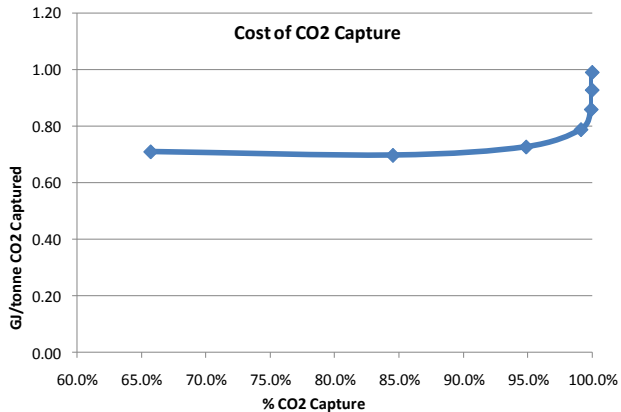
## Cost Comparisons

Levelized cost of energy (LCOE) is the total cost of power generation taking into account fuel, capital (Cap), fixed operating and maintenance (FOM), variable operating and maintenance (VOM), and transport storage and monitoring (TS&M) of CO<sub>2</sub> (See graph). The chart below shows potential increases to the LCOE at a new power plant using different carbon capture technologies. Conservative estimates were used where data given was insufficient for the CCC technology



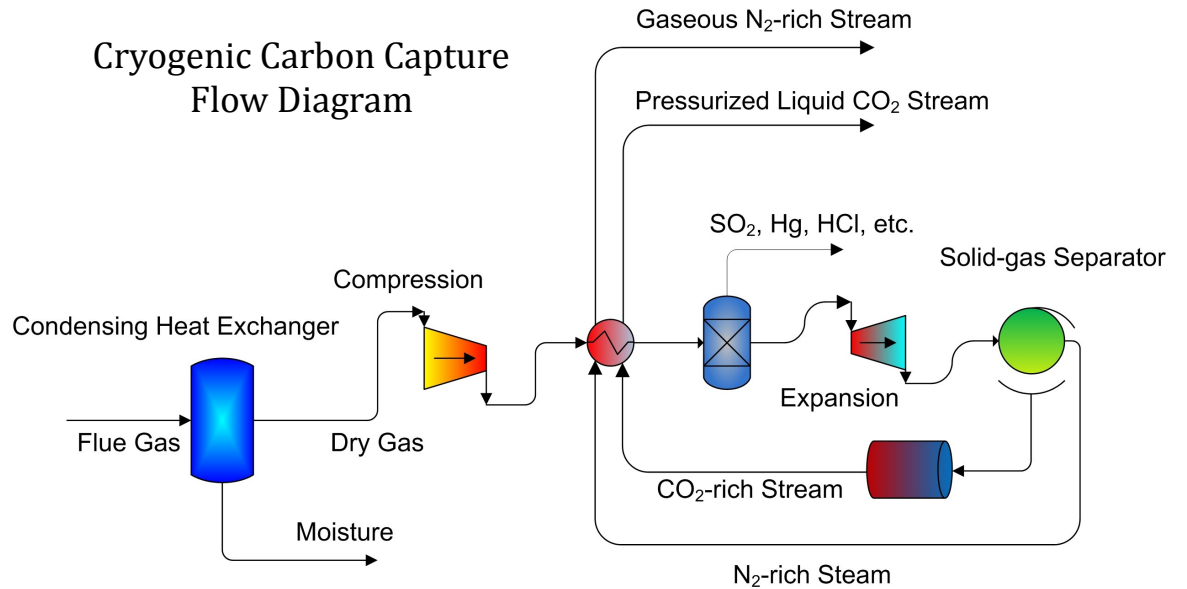
## Energy Efficiency

kJ/ton of CO<sub>2</sub> is a useful measure of the energy efficiencies of these competing carbon-capture processes. Advanced process modeling software was used to generate these numbers.



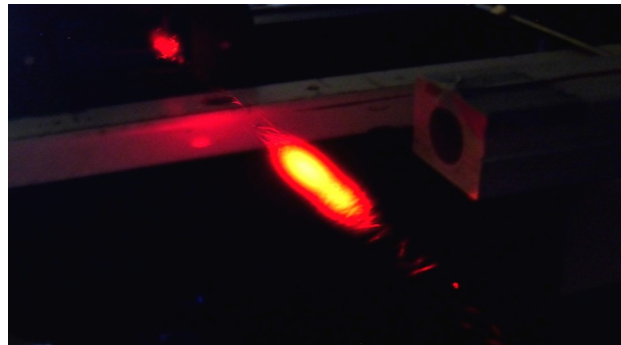
# Cryogenic Carbon Capture

Cryogenic Carbon Capture (CCC) is a patent pending process developed by Dr. Larry Baxter at Brigham Young University. It is designed to separate a nearly pure stream of CO<sub>2</sub> from power plant flue gas. The CCC process is applied post combustion and is suitable for retrofitting existing power plants.



## Process Description

The Cryogenic Carbon Capture (CCC) process dries and cools a flue gas stream, modestly compresses it, and cools it to slightly above the frost point of CO<sub>2</sub>. The gas is then expanded, further cooling the stream and precipitating solid CO<sub>2</sub>. The solid CO<sub>2</sub> is separated from the flue gas and the pure CO<sub>2</sub> stream is pressurized. The cooled CO<sub>2</sub> and N<sub>2</sub> streams are then used in a heat exchanger to cool incoming flue gas. The final result is the CO<sub>2</sub> in a liquid phase and a gaseous nitrogen stream.

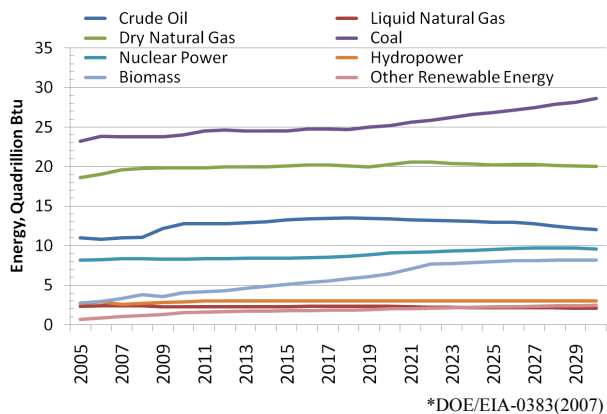


## CO<sub>2</sub> Storage

SES has also developed an innovative geologic storage technology. This technology has the ability to store CO<sub>2</sub> in aquifers at quantities up to 20 times higher than is possible with existing methods. This technology also has the potential to eliminate the risk of a rapid release event.

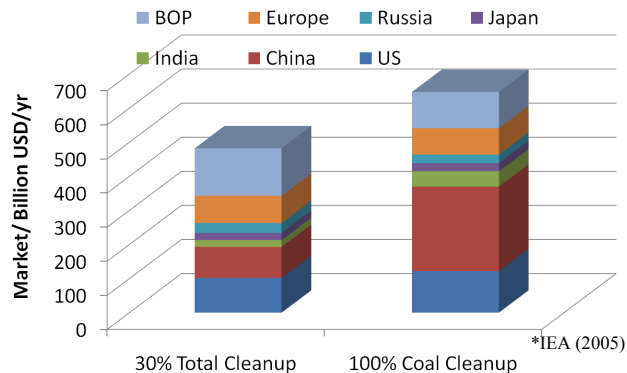
## Energy Projections

Energy projections over the next twenty years show an increase in demand for coal-based energy production (see graph). Carbon regulation, such as cap and trade, already exists in Europe and is expected to spread to the rest of the developed world soon. Given these two facts, carbon capture and storage (CCS) is an important area of research.



## Carbon Capture Sequestration Market

Current cost estimates for competing CCS technologies average over \$50 per ton of CO<sub>2</sub>. Using these estimates, capturing 30% of world CO<sub>2</sub> emissions will cost about \$400B. Capturing all the coal derived CO<sub>2</sub> emissions worldwide would cost over \$650B (see graph). The Cryogenic Carbon Capture (CCC) process drastically reduces this cost, with estimates of around \$33 per ton.



Please contact us:

801-850-6364

[info@sustainablees.com](mailto:info@sustainablees.com)

[www.SustainableES.com](http://www.SustainableES.com)

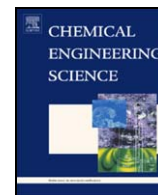
Sustainable Energy Solutions  
242 W 700 S  
Orem, UT 84058

# Sustainable Energy Solutions

ENERGY INNOVATION



[www.SustainableES.com](http://www.SustainableES.com)



## Cryogenic CO<sub>2</sub> capture using dynamically operated packed beds

M.J. Tuinier<sup>a</sup>, M. van Sint Annaland<sup>a,\*</sup>, G.J. Kramer<sup>b</sup>, J.A.M. Kuipers<sup>a</sup>

<sup>a</sup>Faculty of Science and Technology, IMPACT, University of Twente, P.O. Box 217, 7500 AE Enschede, The Netherlands

<sup>b</sup>Shell Global Solutions International B.V., P.O. Box 38000, 1030 BN Amsterdam, The Netherlands

### ARTICLE INFO

#### Article history:

Received 30 June 2008

Received in revised form 15 December 2008

Accepted 29 January 2009

Available online 10 February 2009

#### Keywords:

Separations

CO<sub>2</sub> capture

Phase change

Cryogenic

Packed bed

Dynamic simulation

### ABSTRACT

In this work a novel post-combustion CO<sub>2</sub> capture process concept is proposed and developed, based on cryogenic CO<sub>2</sub> freeze-out in dynamically operated packed beds. When feeding a flue gas containing CO<sub>2</sub>, H<sub>2</sub>O and inert gases to a previously refrigerated packed bed, an effective separation between CO<sub>2</sub>, H<sub>2</sub>O and the permanent gases can be achieved on the basis of differences in dew and sublimation points. Temperature and concentration fronts will develop, which move through the bed with different velocities. H<sub>2</sub>O and CO<sub>2</sub> will condensate and desublimates, respectively, extracting the cold energy stored in the packing and therefore avoiding unacceptable pressure drop or plugging. Great advantage is that both H<sub>2</sub>O and CO<sub>2</sub> can be separated from a flue gas simultaneously, circumventing costly pretreatment steps. Furthermore, no chemical absorbent or elevated pressures are required. Experiments have been carried out and demonstrated that CO<sub>2</sub> can be well separated from N<sub>2</sub>. The process is described by a pseudo-homogeneous 1D model. The resulting simulations show good resemblance with experiments.

© 2009 Elsevier Ltd. All rights reserved.

### 1. Introduction

Reduction of anthropogenic CO<sub>2</sub> emissions is becoming an urgent issue as concerns about global warming are increasing. Energy production processes based on fossil fuels will have to be replaced by new processes using renewable resources, viz. wind, solar, biomass and fusion energy. However, many of these technologies still require much further development, and it is not realistic to assume that our energy production will be switched toward renewables on a short term. It is expected that the world will remain largely dependent on fossil fuels for the next decades (US Department of Energy, 2007) therefore making capture and storage of CO<sub>2</sub> from flue gases a key measure to reduce CO<sub>2</sub> emissions to the atmosphere.

Technologies for CO<sub>2</sub> capture are often classified into oxyfuel, pre- and post-combustion processes. In oxyfuel processes fossil fuels are combusted using pure oxygen, circumventing dilution of CO<sub>2</sub> with nitrogen. In pre-combustion processes fossil fuels are gasified, CO<sub>2</sub> is subsequently captured and hydrogen is fed to the combustion chamber. Post-combustion processes are based on capturing CO<sub>2</sub> from flue gases from conventional air fired power plants. This technology can therefore be retrofitted to already operating power plants and industries. For this reason post-combustion is

considered the most realistic technology on the short term. Several capture processes are currently under development, such as scrubbing with amines (Linde, 1985), pressure swing adsorption (PSA) (Ravikumar and Reddy, 1999) or membrane processes (Powell and Qiao, 2006). All suggested options will result in energy penalties, caused by regeneration of CO<sub>2</sub> loaded absorbents or by recompression of flue gas streams in view of the operation at elevated pressures. State-of-the-art technology is amine solvent scrubbing. Main difficulties for this technology are the stability of the solvents and the energy requirements to strip CO<sub>2</sub> from the loaded solvent.

A relatively novel CO<sub>2</sub> capture technology is based on cryogenic removal of CO<sub>2</sub>. Expensive refrigeration can possibly be avoided when exploiting the cold duty available at liquefied natural gas (LNG) regasification sites. Currently, LNG is being regasified using seawater or by using water baths which are heated by burning a fuel gas (Ertl et al., 2006). The global LNG market is strongly growing (John and Robertson, 2008), therefore integration of LNG regasification and a cryogenic CO<sub>2</sub> capture technology could be beneficial. Great advantages of cryogenic CO<sub>2</sub> capture are that no chemical absorbents are required and that the process can be operated at atmospheric pressures. Clodic and Younes (2002, 2005) have developed a cryogenic CO<sub>2</sub> capture process, where CO<sub>2</sub> is desublimated as a solid onto surfaces of heat exchangers which are cooled by evaporating a refrigerants blend. With calculations and experimental tests they showed that their process could compete with other post-combustion CO<sub>2</sub> capture processes. The main disadvantage of their system is that the water content in the feed stream to the cooling units should be

\* Corresponding author. Tel.: +31 53 489 4478; fax: +31 53 489 2882.

E-mail address: [m.vansintannaland@tnw.utwente.nl](mailto:m.vansintannaland@tnw.utwente.nl) (M. van Sint Annaland).

minimal in order to prevent plugging by ice or an unacceptably high rise in pressure drop during operation. Therefore, several costly steps are required to remove all water traces from the flue gas. In addition the increasing layer of solid CO<sub>2</sub> onto heat exchanger surfaces during the capture cycle will adversely affect the heat transfer, reducing the process efficiency. Moreover, the costly heat exchangers have to be switched to regeneration cycles operated at a different temperature, which should be carried out with great care to avoid excessive mechanical stresses.

In this work, a promising novel cryogenic CO<sub>2</sub> removal process is developed using dynamically operated packed beds, with which the before mentioned drawbacks can be circumvented. The paper is organized as follows. First, the working principle of the concept is explained. Subsequently the experimental setup and numerical model are described. Finally simulations and experiments are compared for N<sub>2</sub>/CO<sub>2</sub> mixtures.

## 2. Concept

When feeding a relatively hot flue gas (at  $T_{in}$ ) containing CO<sub>2</sub>, H<sub>2</sub>O and inert gases (such as N<sub>2</sub>, O<sub>2</sub>, Ar) to an initially uniformly refrigerated packed bed ( $T_0$ ), an effective separation between CO<sub>2</sub>, H<sub>2</sub>O and the permanent gases can be achieved on the basis of differences in dew and sublimation points as schematically illustrated in Fig. 1.

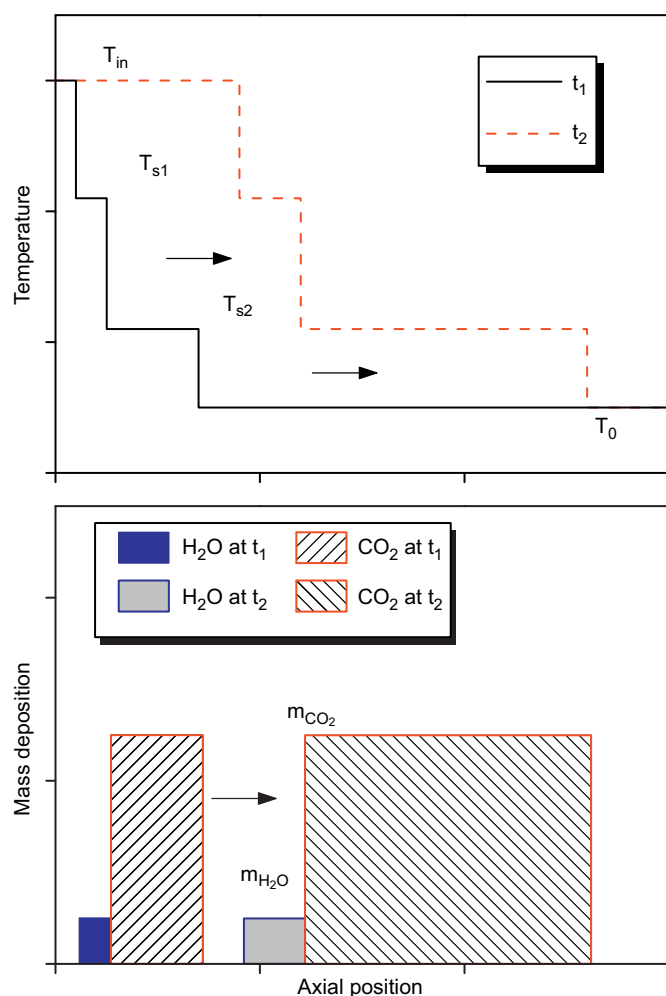


Fig. 1. Typical evolution of axial temperature and condensed/deposited H<sub>2</sub>O/CO<sub>2</sub> mass profiles from  $t_1$  to  $t_2$  when feeding a N<sub>2</sub>/CO<sub>2</sub>/H<sub>2</sub>O gas mixture (at  $T_{in}$ ) to a packed bed refrigerated before uniformly ( $T_0$ ).

The packing material will be heated up and the gas mixture will be cooled down until H<sub>2</sub>O starts to condense. Condensation will take place until the packing material (and the gas phase) will reach an equilibrium temperature ( $T_{s1}$ ). Due to this change in phase, a front of condensing H<sub>2</sub>O will move through the bed toward the outlet of the bed. However, at the same time, the packing material closer to the inlet of the bed will again be heated up from the equilibrium temperature  $T_{s1}$  to the inlet temperature of the gas mixture  $T_{in}$ . This increase in temperature will cause the previously condensed H<sub>2</sub>O to be evaporated again. Therefore another front of evaporating H<sub>2</sub>O will move through the bed toward the outlet of the bed. The velocity of the condensing front is inherently faster than the velocity of the evaporating front, due to the opposed enthalpies involved in the condensation/evaporation. After the water being condensed at the packing surface, the remaining gas mixture will be further cooled until CO<sub>2</sub> starts to desublimates and a new equilibrium temperature ( $T_{s2}$ ) is reached. Based on the same principles, again fronts of sublimating and desublimating CO<sub>2</sub> will develop and move through the bed toward the outlet of the bed. Interestingly, the amount of H<sub>2</sub>O condensed and the amount of CO<sub>2</sub> desublimated per unit volume solid packing reaches a maximum, which is related to the maximum amount of cold stored in the solid packing. Thus, problems with plugging or unacceptable pressure drop increase during the capture cycle can be intrinsically circumvented. This is one of the major advantages of this novel concept with periodically operated packed beds. Another important benefit of this concept is that the outlet gas temperature is at the very minimum temperature of the refrigerant during almost the entire capture cycle, so that the maximum possible CO<sub>2</sub> capture is actually achieved. When the third temperature front reaches the end of the bed, CO<sub>2</sub> will start to break through. At this point, the bed is switched to a regeneration cycle, where a pure gaseous CO<sub>2</sub> flow is used to recover the frosted CO<sub>2</sub>. The heat stored during the capture cycle in the first zone of the bed can now be effectively used to evaporate condensed H<sub>2</sub>O and desublimated CO<sub>2</sub>. When all CO<sub>2</sub> is recovered, the bed is switched to a cooling cycle, where the bed is cooled down using a refrigerated inert gas.

## 3. Experimental setup and procedure

A packed bed was constructed, consisting of a borosilicate glass tube ( $OD \times ID \times L = 40 \times 35 \times 300$  mm) surrounded by a glass vacuum jacket ( $OD \times ID = 60 \times 55$  mm). The tube is packed with spherical glass particles ( $d_p = 4.04$  mm,  $\rho_s = 2547$  kg/m<sup>3</sup>). A flow sheet of the experimental setup is shown in Fig. 2. During cooling cycles the bed was fed with a N<sub>2</sub> gas flow which was refrigerated in a coil positioned in a liquid nitrogen bath. After cooling down the bed, the feed was switched to a N<sub>2</sub>/CO<sub>2</sub> mixture at ambient temperature. The gas feed flow rates were controlled with mass flow controllers (Bronkhorst El-flow). The temperatures in the bed were measured along the bed length in the radial center with 11 thermocouples (Thermo-Electric K-type) at every 3 cm in axial direction. The pressure at the inlet of the bed was measured using an analogue pressure indicator. The CO<sub>2</sub> content in the outlet stream was analyzed with an IR-analyzer (Sick-Maihak, s610, 0–3 vol%). The front of desublimated CO<sub>2</sub> could be visually inspected with a camera.

## 4. Numerical study

The prevailing heat and mass transfer processes in the periodically operated packed beds have been investigated with a pseudo-homogeneous 1D plug flow model with superimposed axial dispersion. The modeling was based on the following main assumptions:

- It is assumed that heat losses to the environment are small (i.e. adiabatic operation) and additionally that a uniform velocity

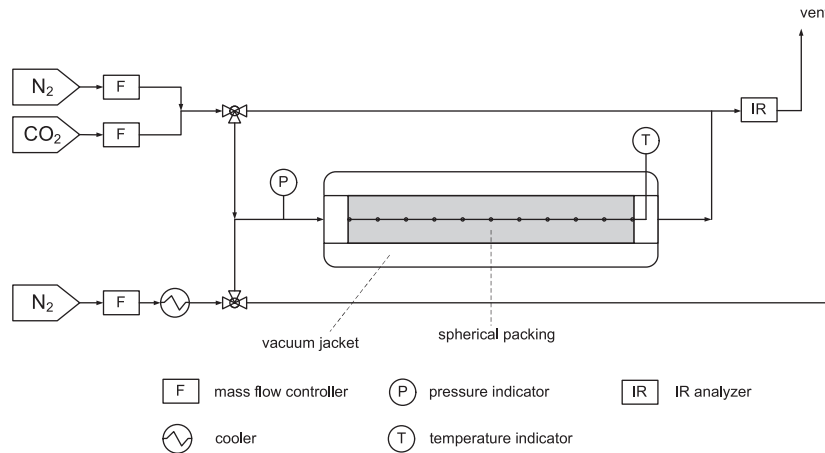


Fig. 2. Flowsheet of the vacuum insulated packed bed.

Table 1

Model equations for the 1D pseudo-homogeneous model.

Component mass balances for the gas phase:
$\varepsilon_g \rho_g \frac{\partial \omega_{i,g}}{\partial t} = -\rho_g v_g \frac{\partial \omega_{i,g}}{\partial z} + \frac{\partial}{\partial z} \left( \rho_g D_{eff} \frac{\partial \omega_{i,g}}{\partial z} \right) - \dot{m}_i' a_s + \omega_{i,g} \sum_{i=1}^{n_c} \dot{m}_i' a_s$
Component mass balance for the solid phase:
$\frac{\partial m_i}{\partial t} = \dot{m}_i' a_s$
Total continuity equation for the gas phase:
$\frac{\partial(\varepsilon_g \rho_g)}{\partial t} = -\frac{\partial(\rho_g v_g)}{\partial z} - \sum_{i=1}^{n_c} \dot{m}_i' a_s$
Energy balance (gas and solid phase):
$(\varepsilon_g \rho_g C_{p,g} + \rho_s (1 - \varepsilon_g) C_{p,s}) \frac{\partial T}{\partial t} = -\rho_g v_g C_{p,g} \frac{\partial T}{\partial z} + \frac{\partial T}{\partial z} \left( \lambda_{eff} \frac{\partial T}{\partial z} \right) - \sum_{i=1}^{n_c} \dot{m}_i' a_s \Delta h_i$

profile exists in the absence of radial temperature and concentration gradients allowing the consideration of the axial temperature and concentration profiles only.

- Possible heat transfer limitations between the solid packing and the bulk of the gas phase were accounted for via effective axial heat dispersion (pseudo-homogeneous model).
- The rate of mass deposition and sublimation of CO<sub>2</sub> was assumed to be proportional to the local deviation from the phase equilibrium, taking a reasonably short equilibration time constant ( $g$ ), which was assumed independent of temperature. The rate of sublimation of previously deposited CO<sub>2</sub> was assumed to approach a first order dependency on the mass deposition when this mass deposition approached zero.

The mass and energy conservation equations have been listed in Table 1. The constitutive equations for the transport parameters and the mass deposition rate have been summarized in Tables 2 and 3, respectively. The gas phase (mixture) properties have been computed according to Reid et al. (1987), using the pure component data supplied by Daubert and Danner (1985). Initial temperature profiles were taken from experiments without any mass deposited onto the solid packing, where the gas phase in the bed was initially N<sub>2</sub>. Furthermore, the usual Danckwerts-type boundary conditions were applied at the inlet and outlet of the beds.

The system of strongly non-linear, coupled partial differential equations was solved using a very efficient finite volume discretization technique, using a second order SDIRK (singly diagonally implicit Runge–Kutta) scheme for the accumulation terms, an explicit

Table 2

Heat and mass transfer coefficients.

Effective axial heat dispersion in a transient packed bed (Vortmeyer and Berninger, 1982):
$\lambda_{eff} = \lambda_{bed,0} + \frac{Re Pr \lambda_g}{Pe_{ax}} + \frac{Re^2 Pr^2 \lambda_g}{6(1 - \varepsilon_g) Nu}$
In which $Pe_{ax}$ is calculated according to Gunn and Misbah (1993):
$Pe_{ax} = \frac{2p}{1-p}, \quad p = 0.17 + 0.33 \exp^{-24/Re}$
$\lambda_{bed,0}$ is calculated according to Zehner and Schlünder (1970)
Gas-to-particle heat transfer coefficient (Gunn, 1978):
$Nu = (7 - 10\varepsilon_g + 5\varepsilon_g^2)(1 + 0.7 Re^{0.2} Pr^{1/3}) + (1.33 - 2.4\varepsilon_g + 1.2\varepsilon_g^2) Re^{0.7} Pr^{1/3}$
Axial mass dispersion (Edwards and Richardson, 1968):
$\frac{D_{eff}}{v_g d_p} = \frac{0.73}{Re Sc} + \frac{0.5}{\varepsilon_g \left( 1 + \frac{9.7 \varepsilon_g}{Re Sc} \right)}$

Table 3

Mass deposition rate.

Mass deposition rate:
$\dot{m}_i' = \begin{cases} g(y_{i,s} p - p_i^\sigma) & \text{if } y_{i,s} p \geq p_i^\sigma \\ g(y_{i,s} p - p_i^\sigma) \frac{m_i}{m_i + 0.1} & \text{if } y_{i,s} p < p_i^\sigma \end{cases}$
Gas–solid equilibrium:
$p_{CO_2}^\sigma(T) = \exp \left( 10.257 - \frac{3082.7}{T} + 4.08 \ln T - 2.2658 \times 10^{-2} T \right)$
$\Delta h_{CO_2}^{sub} = 5.682 \times 10^5 \text{ J/kg}$

fifth order WENO (weighted essentially non-oscillatory) scheme for the convection terms (with implicit first order upwind treatment using the deferred correction method), second order standard implicit central discretization for the dispersion terms and the standard Newton–Raphson technique for the linearly implicit treatment of the source terms. Moreover, automatic time step adaptation and local grid refinement procedures have been implemented, making effective use of the WENO smoothness indicators and interpolation polynomials (Smit et al., 2005). The steep temperature and mass deposition gradients in combination with the strongly non-linear sublimation kinetics require a very efficient and stable numerical implementation using higher order implicit schemes.

In order to demonstrate the model, simulations have been carried out for a capture cycle. A mixture of N<sub>2</sub>, CO<sub>2</sub> and H<sub>2</sub>O (75, 20, 5 vol%, respectively) with an inlet temperature of 100 °C is fed to a

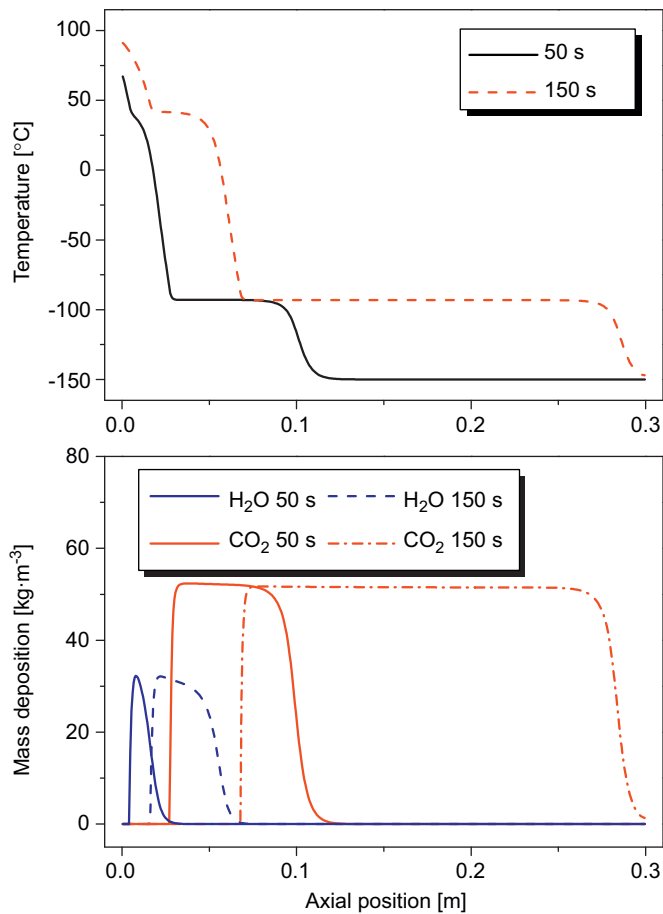


Fig. 3. Simulation of a capture cycle, feeding a  $N_2/CO_2/H_2O$  mixture.

bed which has an uniform initial temperature of  $-150^\circ C$ . The bed dimensions and properties are equal to those described in Section 3. Fig. 3 shows that temperature and mass deposition profiles develop as described before and that  $H_2O$  and  $CO_2$  condense/desublimate at different zones in the bed and that indeed an effective simultaneous separation is obtained.

## 5. Experimental validation

Experiments have been carried out in order to demonstrate the process concept and to validate the developed numerical model. First the bed was cooled using a refrigerated  $N_2$  flow until the bed reached a stationary temperature profile. Due to heat radiation into the system this initial profile is slightly increasing (almost linearly) from the inlet. The temperature difference between the inlet and outlet is typically about  $20^\circ C$ , which is relatively small compared to the temperature difference between the refrigerated bed and the gas being fed during the capture cycle.

When feeding a  $CO_2$  containing gas mixture to the refrigerated packed bed, a moving front of deposited  $CO_2$  was observed visually as depicted in Fig. 4. The axial temperature profiles at several time steps after feeding an ambient  $N_2/CO_2$  mixture containing 20 vol%  $CO_2$  are shown in Fig. 5. After approximately 200 s the second front reached the end of the bed and  $CO_2$  breakthrough was detected in the outlet stream. The  $N_2/CO_2$  mixture is fed through the same inlet tube as the refrigerated  $N_2$  during the cooling cycle. Therefore the temperature of the packing at the inlet does not attain ambient temperatures immediately, but increased slowly as shown in Fig. 5. The experiment was repeated for a feed mixture containing 30 vol%  $CO_2$ .



Fig. 4.  $CO_2$  ice formed at the packing surface during a capture cycle.

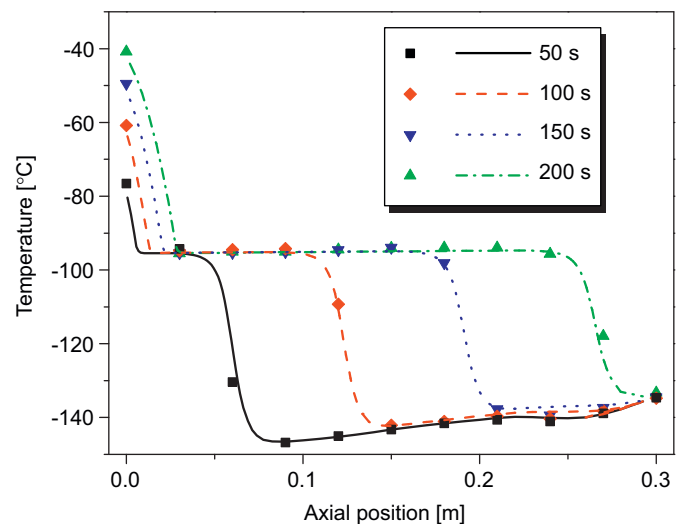


Fig. 5. Experimental (markers) and simulated (lines) evolution of axial temperature profiles  $-y_{CO_2,in} = 0.2$ ,  $\Phi_m = 0.27 \text{ kg/m}^2 \text{ s}$ .

The increased  $CO_2$  inlet concentration resulted in a higher saturation temperature ( $-91.5^\circ C$  versus  $-94.5^\circ C$ ) and therefore the packing storage capacity slightly increased. However, due to the higher molar  $CO_2$  feed flow rate, the front velocity of the second temperature front increased. Fig. 6 shows that  $CO_2$  breakthrough already occurred after 150 s.

The experimental results have been studied with simulations using identical operating conditions, where the experimentally determined initial temperature profiles of the bed were taken as the initial condition in the model. The inlet transient temperatures are also taken from measurements at the inlet of the bed.

As no information on the sublimation rates is available in literature, the equilibrium time constant ( $g$ ) was determined by comparing simulation results with the experimental findings. Fig. 7 shows the effect of  $g$  on the outlet temperature and outlet  $CO_2$  volume fraction in time. It can be observed that experimental results are best described when using a constant of about  $1 \times 10^{-6} \text{ s/m}$ . Axial profiles resulting from simulations using this equilibrium time constant are depicted in Figs. 5 and 6. It is shown that front evolution can be very well described by the developed model.

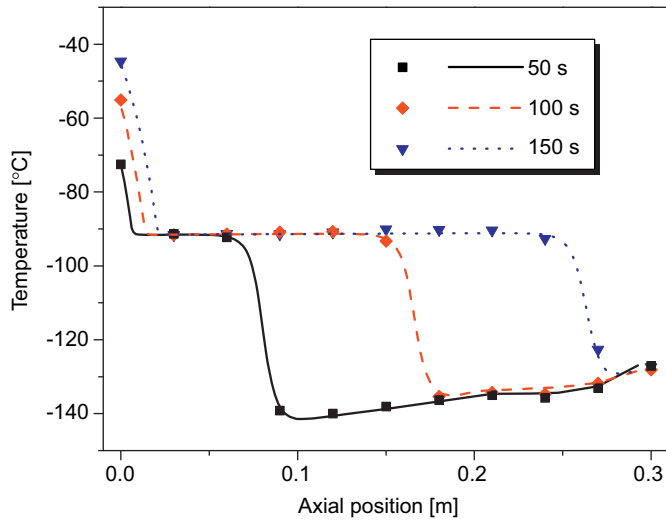


Fig. 6. Experimental (markers) and simulated (lines) evolution of axial temperature profiles— $y_{\text{CO}_2,\text{in}} = 0.3$ ,  $\Phi_m'' = 0.28 \text{ kg/m}^2 \text{ s}$ .

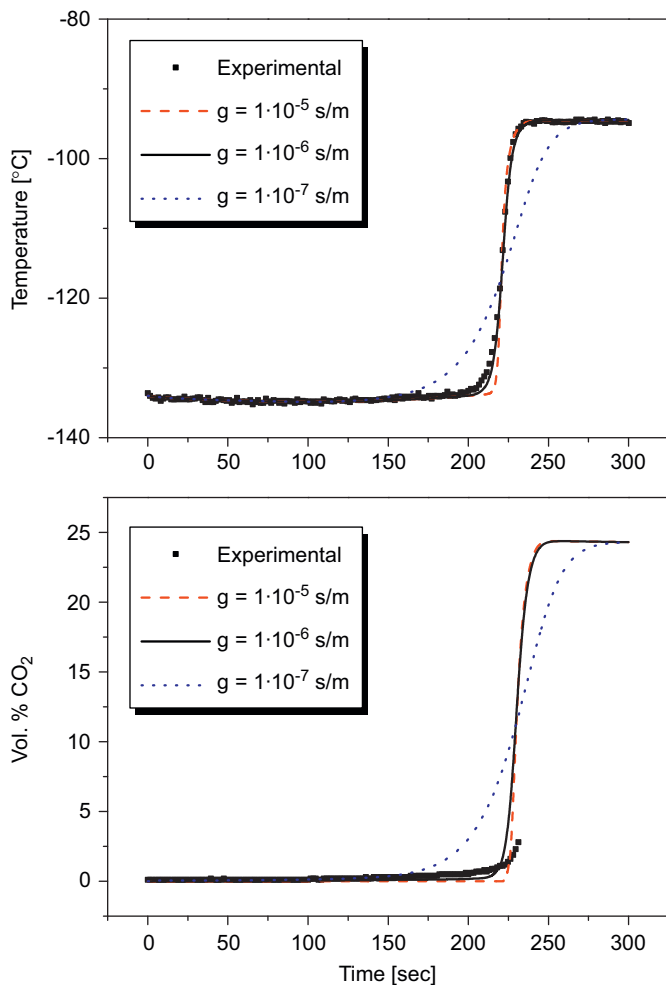


Fig. 7. Outlet temperature and  $\text{CO}_2$  vol% from experiments (markers) and simulations (lines) using different equilibrium time constants ( $g$ )— $y_{\text{CO}_2,\text{in}} = 0.2$ ,  $\Phi_m'' = 0.27 \text{ kg/m}^2 \text{ s}$ .

## 6. Discussion and conclusions

A novel process for cryogenic  $\text{CO}_2$  freeze-out using dynamically operated packed beds has been proposed and the basic working principle has been demonstrated experimentally for  $\text{N}_2/\text{CO}_2$  mixtures. An effective separation on the basis of differences in dew and sublimation points can be achieved without increasing pressure drops or plugging problems. The temperature and concentration fronts moving through the bed can be very well described with a 1D homogeneous model. In addition, detailed simulations have been carried out for  $\text{N}_2/\text{CO}_2/\text{H}_2\text{O}$  mixtures, demonstrating that an effective simultaneous separation between  $\text{CO}_2$  and  $\text{H}_2\text{O}$  can be achieved. Future work will focus on the experimental validation of the concept and model for  $\text{H}_2\text{O}$  containing flue gases and the determination of more detailed sublimation kinetics. Moreover, a pilot plant will be constructed in which capture, recovery and cooling cycles will be operated in parallel to provide an integral proof of principle of the process.

## Notation

$a_s$	specific solid surface area, $\text{m}^2/\text{m}^3$
$C_p$	heat capacity, $\text{J}/\text{kg}/\text{K}$
$d_p$	particle diameter, m
$D$	diffusion coefficient, $\text{m}^2/\text{s}$
$D_{\text{eff}}$	effective diffusion coefficient, $\text{m}^2/\text{s}$
$g$	mass deposition rate constant, $\text{s}/\text{m}$
$ID$	inner diameter, mm
$L$	bed length, mm
$m_i$	mass deposition of component $i$ per unit bed volume, $\text{kg}/\text{m}^3$
$m_i''$	mass deposition rate per unit surface area for component $i$ , $\text{kg}/\text{m}^2/\text{s}$
$n_c$	number of components, dimensionless
$Nu$	Nusselt number ( $\alpha_{gs}d_p/\lambda_g$ )
$OD$	outer diameter, mm
$p$	parameter in axial heat dispersion coefficient
$p$	pressure, Pa
$Pe_{ax}$	Peclet number for axial heat dispersion ( $\rho_g v_g d_p C_{p,g}/\lambda_{ax}$ )
$Pr$	Prandtl number ( $C_{p,g}\eta_g/\lambda_g$ )
$Re$	Reynolds number ( $\rho_g v_g d_p/\eta_g$ )
$Sc$	Schmidt number ( $\eta_g/\rho_g D$ )
$t$	time, s
$T$	temperature, K, $^{\circ}\text{C}$
$v$	superficial velocity, m/s
$y$	mole fraction, mol/mol
$z$	axial coordinate, m

## Greek letters

$\alpha_{gs}$	heat transfer coefficient solids–gas bulk, $\text{W}/\text{m}^2/\text{K}/\text{s}$
$\Delta h_i$	enthalpy change related to the phase change of component $i$ , $\text{J}/\text{kg}$
$\epsilon_g$	bed void fraction, dimensionless
$\lambda$	thermal conductivity, $\text{W}/\text{m}/\text{K}/\text{s}$
$\lambda_{ax}$	axial thermal conductivity, $\text{W}/\text{m}/\text{K}/\text{s}$
$\lambda_{bed,0}$	effective bed conductivity at no flow conditions, $\text{W}/\text{m}/\text{K}/\text{s}$
$\lambda_{\text{eff}}$	effective conductivity, $\text{W}/\text{m}/\text{K}/\text{s}$
$\rho$	density, $\text{kg}/\text{m}^3$
$\Phi_m''$	mass flux, $\text{kg}/\text{m}^2/\text{s}$
$\omega$	mass fraction, $\text{kg}/\text{kg}$

## Subscripts

0	initial
g	gas phase

<i>i</i>	component <i>i</i>
<i>in</i>	inlet
<i>s</i>	solid phase
S1	H <sub>2</sub> O equilibrium
S2	CO <sub>2</sub> equilibrium

#### Superscripts

$\sigma$	equilibrium
----------	-------------

#### Acknowledgment

Shell Global Solutions International is kindly acknowledged for their financial support.

#### References

- Clodic, D., Younes, M., 2002. A new method for CO<sub>2</sub> capture: frosting CO<sub>2</sub> at atmospheric pressure. In: Sixth International Conference on Greenhouse Gas Control Technologies, GHGT6, Kyoto, October 2002, pp. 155–160.
- Clodic, D., Younes, M., 2005. CO<sub>2</sub> capture by anti-sublimation—thermo-economic process evaluation. In: Fourth Annual Conference on Carbon Capture & Sequestration, Alexandria, USA, 2–5 May 2005.
- Daubert, T.E., Danner, R.P., 1985. Data Compilation Tables of Properties of Pure Compounds. American Institute of Chemical Engineers, New York.
- Edwards, M.F., Richardson, J.F., 1968. Gas dispersion in packed beds. *Chemical Engineering Science* 23, 109–123.
- Ertl, B., Durr, C., Coyle, D., Mohammed, I., Huang, S., 2006. New, LNG receiving terminal concepts. In: World Petroleum Congress Proceedings.
- Gunn, D.J., 1978. Transfer of heat or mass to particles in fixed and fluidized beds. *International Journal of Heat and Mass Transfer* 21 (4), 467–476.
- Gunn, D.J., Misbah, M.M.A., 1993. Bayesian estimation of heat transport parameters in fixed beds. *International Journal of Heat and Mass Transfer* 36 (8), 2209–2221.
- John, A., Robertson, S., 2008. LNG: world: strong growth forecast for global LNG expenditure. *Petroleum Review* 62 (732), 34–35.
- Linde, G., 1985. Process for separation of CO<sub>2</sub> from CO<sub>2</sub> containing gases. By LINDE AG. US 4528002.
- Powell, C.E., Qiao, G.G., 2006. Polymeric CO<sub>2</sub>/N<sub>2</sub> gas separation membranes for the capture of carbon dioxide from power plant flue gases. *Journal of Membrane Science* 279 (1–2), 1–49.
- Ravikumar, R., Reddy, S., 1999. Recovery of CO<sub>2</sub> and H<sub>2</sub> from PSA offgas in a H<sub>2</sub> plant. By Fluor Corp. WO 00/27505.
- Reid, R.C., Prausnitz, J.M., Poling, B.E., 1987. *The Properties of Gases and Liquids*, fourth ed. McGraw-Hill, Inc., New York.
- Smit, J., van Sint Annaland, M., Kuipers, J.A.M., 2005. Grid adaptation with WENO schemes for non-uniform grids to solve convection-dominated partial differential equations. *Chemical Engineering Science* 60, 2609–2619.
- US Department of Energy, 2007. Energy Information Administration International Energy Outlook 2007.
- Vortmeyer, D., Berninger, R., 1982. Comments on the paper 'Theoretical prediction of effective heat transfer parameters in packed beds' by Anthony Dixon and D.L. Cresswell [A.I.Ch.E. J. 25, 663, 1979]. *A.I.Ch.E. Journal* 28 (3), 508–510.
- Zehner, P., Schlünder, E.U., 1970. Thermal conductivity of granular materials at moderate temperatures. *Chemie Ingenieur Technik* 42, 933–941.